



A spin-state-selective experiment for measuring heteronuclear one-bond and homonuclear two-bond couplings from an HSQC-type spectrum

Perttu Permi*

Institute of Biotechnology, NMR Laboratory, P.O. Box 56, University of Helsinki, FIN-00014, Helsinki, Finland

Received 20 August 2001; Accepted 13 November 2001

Key words: dipolar couplings, HSQC, NMR, proteins, scalar couplings, side-chains, spin-state-selection

Abstract

Recently, a set of selective 1D experiments with spin-state-selective excitation for CH spin systems was introduced by Parella and Belloc (*J. Magn. Reson.*, **148**, 78–87 (2001)). We have expanded and generalized this concept further, and demonstrated that a very simple experiment utilizing spin-state-selective filtering can be used for simultaneous measurement of heteronuclear $^1J_{\text{NH}}$ (or $^1J_{\text{CH}}$) and geminal $^2J_{\text{HH}}$ couplings from two-dimensional ^{15}N - ^1H (or ^{13}C - ^1H) correlation spectrum. The experiment has very high sensitivity owing to the preservation of equivalent coherence transfer pathways analogous to the sensitivity and gradient enhanced HSQC experiment. However, overall length of the pulse sequence is $1/(2J)$ shorter than the gradient selected SE-HSQC experiment. Furthermore, the spin-state-selection can be utilized between NH and NH_2 (or CH and CH_2) moieties by changing the phase of only one pulse. The pulse scheme will be useful for the measurement of scalar and residual dipolar couplings in wide variety of samples, due to its high sensitivity and artifact suppression efficiency. The method is tested on NH_2 and CH_2 moieties in ^{15}N - and $^{15}\text{N}/^{13}\text{C}$ -labeled ubiquitin samples.

Introduction

In recent years, by introduction of residual dipolar couplings, transverse relaxation optimized spectroscopy (TROSY) and spin-state-selection (S^3), NMR of biological macromolecules has taken major leap towards the structure determination of larger proteins and macromolecular complexes. Especially residual dipolar couplings have proven to be rich source of structural and dynamic information (Tolman et al., 1995; Tjandra and Bax, 1997; Bax and Tjandra, 1997; Annila et al., 1999; Prestegard et al., 2000). Several methods have been devised for precise measurement of dipolar couplings not only along the protein backbone (Yang et al., 1998, 1999; Ottiger et al., 1998a; Permi et al., 2000a), but side-chains as well (Ottiger et al., 1998b; Permi et al., 1999a, 2000a; Carlmagno et al., 2000; Otting et al., 2000; Tjandra et al., 2000; Kaikkonen and Otting, 2001;

Chou and Bax, 2001; Kontaxis and Bax, 2001; Mittermaier and Kay, 2001). It is of particular interest to measure several dipolar couplings per amino acid residue because an extensive set of different couplings yield more precise values for polar angles, thus improving the precision of the structure (Permi et al., 2000a). Spin-state-selection (Yang and Nagayama, 1996; Meissner et al., 1997), i.e., the filtering scheme that manipulates the desired coherences in order to produce multiplet patterns showing only α - or β -state of coupled spins, has been widely employed for the measurement of scalar and residual dipolar couplings (Ottiger et al. 1998a; Yang et al. 1998; Permi et al., 1999a–c, 2000a,b). Spin-state-selective excitation is also essential part of the TROSY approach (Pervushin et al., 1997). Moreover, the editing with respect to spin-states can also be used for suppression of diagonal signals (Pervushin et al., 1999), and to distinguish between the intra- and inter-residual connectivities in the HNCA experiment for the assignment purposes in very large proteins (Permi and Annila, 2001). We have previously shown that the spin-state-selective TROSY

*To whom correspondence should be addressed. E-mail: Perttu.Permi@helsinki.fi

experiments allow precise and convenient measurement of nine different dipolar couplings in protein main-chain (Permi and Annala, 2000; Permi et al., 2000a). In order to obtain information of side-chain orientation, and potential dynamic information, it is of utmost importance to measure several dipolar couplings in side-chains also. One of the major obstacles has been the measurement of heteronuclear one-bond couplings and homonuclear two-bond couplings in I_2S , especially methylene, system. Several techniques have been employed for this purpose. Heteronuclear one-bond couplings in I_2S moieties have been formerly determined from the DQ/ZQ splittings (Permi et al., 1999a), from the SPITZE-HSQC experiment (Carlomagno et al., 2000), or more recently, derived from the sum of the two $^1J_{CH}$ couplings by the fitting procedure (Chou and Bax, 2001). Homonuclear two-bond couplings can be measured from the DQ/ZQ splittings (Permi et al., 1999) or from the E.COSY pattern in very sophisticated SPITZE-HSQC, or in the case of plain sign determination, from the homonuclear antiphase multiplet (Otting et al., 2000). The geminal H-H couplings can also be measured using the α/β -HSQC experiment (Sattler et al., 1996), which selectively polarizes either α or β lines of arising doublet due to the geminal coupling. In this paper we show that exceptionally simple spin-state-selective experiment can be used for convenient and simultaneous measurement of two heteronuclear one-bond couplings and the geminal coupling between two protons in the NH_2 and CH_2 moieties. The same pulse sequence can be used for measuring one-bond couplings from spin-state-selective spectra in the IS spin system by simply changing the phase of a single 90° pulse.

Description of the pulse sequence

The work presented in this paper is a modification of the idea originally presented by Parella and Belloc (Parella and Belloc, 2001). The authors show that the spin-state-selection in the IS moiety can be achieved with full sensitivity in the carbon-selective, gradient-enhanced 1D HMQC/HSQC experiments, by incorporating a single hard ^{13}C pulse (S^3 pulse) into the pulse sequence (Parella and Belloc, 2001). Further elaboration of this approach reveals that a very simple modification of the original scheme enables measurement of one-bond couplings $^1J_{IS}$, and the geminal proton-proton coupling in the I_2S moieties.

The pulse sequence for measuring $^1J_{IS}$, and $^1J_{I^1S}$, $^1J_{I^2S}$ and $^2J_{I^1I^2}$ couplings from two-dimensional I-S correlation spectrum is presented in Figure 1. The pulse scheme is two-dimensional extension, with a few modifications, of the experiment presented by Parella and Belloc. For simplicity, let us first focus on an IS system, where I is the proton, directly bound heteronucleus S, typically ^{15}N or ^{13}C spin. Initially, the magnetization is transferred from the spin I to the spin S by the usual INEPT step. Subsequently, the chemical shift of the S spin is first recorded during t_1 , and then the ensuing gradient pulse labels the desired coherence. Thus, the relevant density operators at time point a can be described by $I_z S_y \cos(\omega_S t_1) + I_z S_x \sin(\omega_S t_1)$. The influence of the labeling gradient to these coherences are omitted for simplicity because the phase-modulated magnetization is ultimately rephased by the refocusing gradient in an analogous way to sensitivity-enhanced, gradient-selected HSQC (Kay et al., 1992). After chemical shift evolution of the S spin, the desired coherence is transformed back to the proton single quantum coherence, which will refocus during the back-INEPT step, yielding the $I_x \cos(\omega_S t_1)$ coherence prior to detection. The multiple quantum term, $I_y S_x \sin(\omega_S t_1)$ is ultimately transformed to the antiphase $I_y S_z \sin(\omega_S t_1)$ coherence by an application of 90°_y pulse on the S spin (time point b). Whether this pulse is applied from y, or $-y$ axis, the I^-S^a , or I^-S^b coherence will be selected. Thus, the proposed pulse sequence is applicable to measurement of the $^1J(+^1D)_{NH}$ and $^1J(+^1D)_{CH}$ couplings in the IS moieties in the same way as with the other spin-state-selective experiments.

Now, let us consider a three-spin system I^1I^2S , where I^1 and I^2 are two protons bound to same heteronucleus S. The desired magnetization at time point a can now be described by the density operators $I^1_z S_y \cos(\omega_S t_1) + I^1_z S_x \sin(\omega_S t_1)$, and $I^2_z S_y \cos(\omega_S t_1) + I^2_z S_x \sin(\omega_S t_1)$. Again, the effect of labeling gradient is neglected for the sake of clarity. Two simultaneous 90° pulses on I and S convert the relevant density operators to the $I^1_y S_z \cos(\omega_S t_1)$, $I^1_y S_x \sin(\omega_S t_1)$, $I^2_y S_z \cos(\omega_S t_1)$ and $I^2_y S_x \sin(\omega_S t_1)$ coherences. The antiphase operators $I^1_y S_z \cos(\omega_S t_1)$ and $I^2_y S_z \cos(\omega_S t_1)$ refocus to the in-phase $I^1_x \cos(\omega_S t_1)$ and $I^2_x \cos(\omega_S t_1)$ coherences during the back-INEPT. However, the multiple quantum terms $I^1_y S_x \sin(\omega_S t_1)$ and $I^2_y S_x \sin(\omega_S t_1)$ dephase to the $I^1_y I^2_z S_y \sin(\omega_S t_1)$ and $I^1_z I^2_y S_y \sin(\omega_S t_1)$ coherences. If we now apply an $90^\circ(\hat{S})$ pulse with the phase x, these operators are converted to the dou-

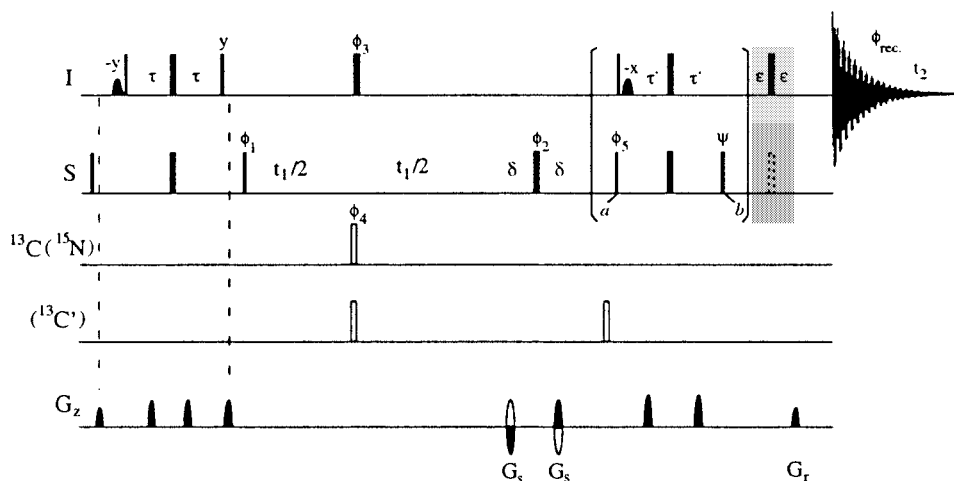


Figure 1. The spin-state-selective pulse sequence, (S^3 - I_2S)-HSQC for determination of scalar and residual dipolar one-bond ^{15}N - $^1\text{H}^1$, (^{15}N - $^1\text{H}^2$ and two-bond $^1\text{H}^1$ - $^1\text{H}^2$) couplings from two-dimensional ^{15}N - ^1H correlation spectra if $S = ^{15}\text{N}$, or one-bond ^{13}C - $^1\text{H}^1$, (^{13}C - $^1\text{H}^2$ and two-bond $^1\text{H}^1$ - $^1\text{H}^2$) couplings from 2D ^{13}C - ^1H HSQC spectra if $S = ^{13}\text{C}$. Narrow (wide) bars denote 90° (180°) pulses, with phase x unless otherwise specified. Half-ellipses describe water selective 90° pulses to obtain water flip-back (Grzesiek and Bax, 1993), which are applied only if $S = ^{15}\text{N}$. The ^1H and ^{15}N carrier positions are 4.7 (water) and 120 (center of ^{15}N spectral region). If $S = ^{15}\text{N}$, the 180° ^{13}C pulse is applied (100 ppm, center of ^{13}C spectral region) during t_1 in order to remove ^{13}C - ^{15}N couplings. If $S = ^{13}\text{C}$, the ^{13}C carrier is set to 35 ppm (center of aliphatic ^{13}C spectral region) in order to avoid excitation of carbonyl resonances, and ^{15}N pulse and $^{13}\text{C}'$ (176 ppm, center of $^{13}\text{C}'$ spectral region, in order to avoid excitation of aliphatic carbons) pulses are applied as shown. The delays employed are: $\tau = 1/(4J_{IS})$; $\tau' = 1/(8J_{IS}) - 1/(4J_{IS})$; δ and ϵ are gradient + field recovery delays. Phase cycling: $\phi_1 = x, -x$; $\phi_2 = 2(x), 2(y), 2(-x), 2(-y)$; $\phi_3 = \phi_4 = 8(x), 8(-x)$; $\phi_5 = x$; $\phi_{\text{rec}} = x, 2(-x), x$. In the case of I_2S groups, the phase setting $\psi = x$, gives the doublet with splitting equal to $^1J_{IS} + ^2J_{II}$, whereas the phase setting $\psi = -x$ gives the doublet with splitting equal to $^1J_{IS} + ^2J_{II}$, leaving the IS moieties unaffected. If $\psi = y$, the spectrum showing only the downfield component of $^1J_{IS}$ doublet results, if $\psi = -y$, the upfield component is selected for IS moieties, whereas I_2S moieties are not affected by this pulse. For the I_2S moieties, additional spin-state-selective filtering can be utilized by setting the delay 2ϵ to $1/(2J_{IS})$ (shaded box), and recording two additional spectra (i.e., for both phase settings of ψ) with and without 180° editing pulse on ^{15}N (dashed rectangular). Consequently, the in- and antiphase spectra are generated that can be added or subtracted during data manipulation to yield only one multiplet component per subspectrum. Frequency discrimination in F_1 is obtained using the sensitivity-enhanced gradient selection (Kay et al., 1992). The echo and antiecho signals are collected separately by inverting the sign of the G_s gradient pulses together with the inversion of ϕ_5 . In addition to echo/anti-echo selection, ϕ_1 and ϕ_{rec} are incremented according to States-TPPI protocol (Marion et al., 1989). Pulsed field gradients are inserted as indicated for coherence transfer pathway selection and residual water suppression. Gradient strengths and durations, for $S = ^{15}\text{N}$, are $G_s = 1.25$ ms (13 G cm^{-1}) and $G_r = 0.250$ ms (13 G cm^{-1}). In the case of $S = ^{13}\text{C}$, $G_s = 0.8$ ms (13 G cm^{-1}) and $G_r = 0.4$ ms (13 G cm^{-1}).

ble antiphase magnetization, described by the density operators $I_y^1 I_z^2 S_z \sin(\omega_S t_1)$ and $I_z^1 I_y^2 S_z \sin(\omega_S t_1)$ (time point b). On the other hand, if the 90° (S) pulse is applied with the phase $-x$, the operators are converted to the $-I_y^1 I_z^2 S_z \sin(\omega_S t_1)$ and $-I_z^1 I_y^2 S_z \sin(\omega_S t_1)$ coherences.

The superposition of these terms is schematically presented in Figure 2. Thus, $I_x^1 \cos(\omega_S t_1)$ ($I_x^2 \cos(\omega_S t_1)$) is in-phase with respect to the S and I^2 spins (S and I^1). If the phase of the last 90° (S) pulse is x , the outer lines of the doublet of doublets are observed with a multiplet component separation equaling to $^1J_{I^1S} + ^2J_{I^1I^2}$ ($^1J_{I^2S} + ^2J_{I^2I^1}$) (spectrum A). If the phase of the pulse is $-x$, the inner lines of the doublet of doublets are selected, and consequently, a splitting equaling to $^1J_{I^1S} - ^2J_{I^1I^2}$ ($^1J_{I^2S} - ^2J_{I^2I^1}$) is observed (spectrum B). It is now obvious that $^1J_{I^1S}$

($^1J_{I^2S}$) can be determined from the cross peak separation between two spectra. Thus, the heteronuclear one-bond coupling between the spins I and S can be determined by measuring peak separation between two spectra, i.e. the separation of $\beta\alpha$ and $\beta\beta$ (or $\alpha\alpha$ and $\alpha\beta$) spin-states is equal to $^1J_{I^1S}$. The same holds true for the $^1J_{I^2S}$, provided that two protons are not degenerate. Analogously, the separation of $\beta\alpha$ and $\alpha\alpha$ (or $\beta\beta$ and $\alpha\beta$) spin-states between two subspectra gives the size of homonuclear two-bond coupling, $^2J_{HH}$. In practice, however, the heteronuclear coupling should be measured from the midpoints of $\beta\alpha$ and $\alpha\alpha$, and $\beta\beta$ and $\alpha\beta$ peaks in order to minimize influence of cross-correlation on determined couplings (*vide infra*).

It is immediately apparent that outcome of the proposed method is somewhat related to the double/zero quantum (DQ/ZQ) spectroscopy (Braun-

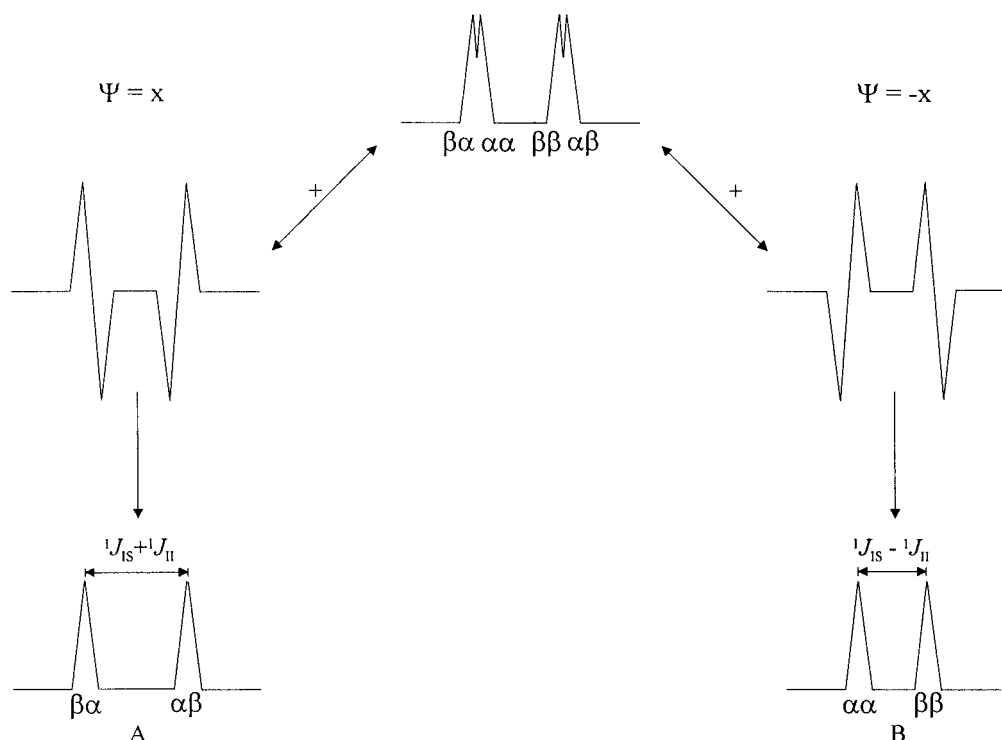


Figure 2. A schematic presentation of arising multiplet pattern in I_2S moieties with respect to the pulse phase ψ . If the last $90^\circ(S)$ pulse is applied with phase x , the multiple quantum term $I_y^1 I_z^2 S_y$ will be converted to observable $I_y^1 I_z^2 S_z$ coherence and its superposition with the in-phase I_x^1 coherence results in spectrum A. When this pulse is applied with phase $-x$, the $I_y^1 I_z^2 S_y$ coherence will be transformed to $-I_y^1 I_z^2 S_z$ coherence. The superposition of the I_x^1 and $-I_y^1 I_z^2 S_z$ coherences results in spectrum B.

schweiler et al., 1983) where two spins, being in the multiple quantum state, couple to the common passive spin. The resulting DQ/ZQ spectrum has a certain desired property; the DQ splitting is the sum of two passive couplings, whereas ZQ splitting is the difference. Hence, the sign and magnitude of two couplings can be inferred by comparing DQ and ZQ splittings. However, the undesired multiple quantum chemical shifts do make the assignment of the spectrum more tedious. In the proposed approach, the dipolar contribution to splitting can be retrieved by comparing data recorded in isotropic phase with the data recorded in anisotropic phase. The large $^1J_{IS}$ coupling is always positive for the $^1J_{CH}$ whereas it is negative for $^1J_{NH}$. Thus, direct comparison of $\beta\alpha$ and $\beta\beta$ (or $\alpha\alpha$ and $\alpha\beta$) spin-states in water, and in the presence of a dilute liquid crystal, gives the sign and magnitude of residual dipolar coupling $^1D_{IS}$. The homonuclear coupling can be measured from cross peak displacement between $\beta\alpha$ and $\alpha\alpha$ (or $\beta\beta$ and $\alpha\beta$) spin-states.

Experimental

The experimental verification was carried out with two samples: 1.0 mM, uniformly ^{15}N -labeled ubiquitin, dissolved in 90/10% H_2O/D_2O in Wilmad 535PP NMR tube, pH = 4.7 at $30^\circ C$, and 0.8 mM $^{13}C/^{15}N$ -labeled ubiquitin, in 90/10% H_2O/D_2O in 250 ml Shigemi micro-cell, pH = 4.7 at $30^\circ C$. The corresponding sum and difference spectra were recorded on a Varian Unity INOVA 800 MHz NMR spectrometer, equipped with a triple-resonance and an actively shielded triple-axis pulsed field gradient probehead. Spectra were processed using the standard VNMR 6.1 software package (Varian associates, 1998).

The (S^3-NH_2) -HSQC spectra were recorded in an interleaved manner with 128 and 1024 complex points using 2 transients per FID, which corresponds to acquisition times of 56.8 and 128 ms in t_1 and t_2 , respectively, and giving experimental time of ca. 8 min per spectrum. Data were zero-filled to 1024×4096 data matrices and apodized with shifted squared sine-bell functions in both dimensions.

Experimental parameters for the (S^3 -CH₂)-HSQC experiment: Two spectra, with phase settings $\psi = x$ and $\psi = -x$, were recorded in an interleaved manner with 256 and 1280 complex points using 8 transients per FID, corresponding to acquisition times of 12.2 and 128 ms in t_1 and t_2 , respectively (experimental time of ca. 1.25 h per spectrum). Data were zero-filled to 1024×4096 data matrices and apodized with shifted squared sine-bell functions in both dimensions. The F₂-coupled ¹³C-HSQC spectrum was recorded using the same parameters.

Results and discussion

The new method for measuring $^1J_{IS}$ and $^2J_{II}$ couplings is subject to following considerations. Because the method obtains spin-state-selection without post-processing of the in-phase and antiphase data sets, a possible undesired multiplet component cannot be removed by scaling, i.e., by taking appropriate linear combinations of the in-phase and antiphase data sets (Ottiger et al., 1998a; Meissner et al., 1998). The filter is, although, quite insensitive to J mismatch as well as cross-correlation effects. In fact, the doubly antiphase $I_y^1 I_z^2 S_z$ coherence has the same sine dependence on $^1J(+^1D)_{IS}$ as the in-phase I_x^1 coherence has. However, the I_x^1 coherence has $\sin(\pi^1(J+D)_{IS} 2\Delta')$ dependence, whereas the $I_y^1 I_z^2 S_z$ has $\sin(\pi^1(J+D)_{IS} 2\Delta')$ dependence on signal intensity. Difference between the relaxation rates of proton single quantum coherence ($\exp(-2\Delta'R_{2,SQ})$) and ¹H-¹⁵N (or ¹H-¹³C) multiple quantum coherence ($\exp(-2\Delta'R_{2,MQ})$) will have an influence on the filtering quality. This will lead into an interesting situation: both the in-phase and antiphase coherence have sine dependence on active coupling, thus, the length of the filter can be varied without affecting the relative coherence transfer efficiencies for conversions from $I_y^1 S_z \cos(\omega_S t_1)$ to $I_x^1 \cos(\omega_S t_1)$, and from $I_y^1 S_x \sin(\omega_S t_1)$ to $I_y^1 I_z^2 S_z \sin(\omega_S t_1)$ provided that $^1J_{I_1S}$ and $^1J_{I_2S}$ are comparable in size. It is now obvious that in order to equalize intensity imbalance due to dissimilar relaxation rates, we have an option to shorten the filter. Of course, if the magnitude of $^1J_{I_1S}$ differs drastically from $^1J_{I_2S}$, the cancellation of the undesired multiplet components is not complete, the situation that is typical for ordinary spin-state-selective filters as well (Meissner et al., 1997; Andersson et al., 1998; Ottiger et al., 1998a; Permi et al., 1999b,c). This feature has crucial impact on editing in CH₂ sites. For instance, let us consider

editing in C^β site in methionine. Besides the probable discrepancy in the relaxation rates of ¹H SQ and ¹H-¹³C MQ, the intensity of $I_y^1 S_x$ term scales down by $\cos(2\pi J_{C^\alpha C^\beta} \tau') \cos(2\pi J_{C^\beta C^\gamma} \tau')$ due to the J modulation to mutual aliphatic carbons, C^α and C^γ. It is possible to selectively refocus C^β without inverting the C^α spin during the filter. Hence, we are left with only one coupling partner, C^γ, which has smaller influence on the intensity of arising doubly antiphase component, originating from multiple quantum coherence transfer pathway. However, more versatile approach is to reduce the filter length. This will not have an effect on relative coherence transfer efficiencies of the two terms with respect to the active coupling (*vide supra*), but instead, it reduces the intensity imbalance between these two coherences due to the differential relaxation. More importantly, it will eliminate the effect of passive couplings. The shortcoming is, of course, the possible decrease in overall sensitivity. For methylene sites this is not utmost importance, because the use of shorter filter is practical anyway, owing to the rapid transverse relaxation. For IS moieties, the latter prescription, i.e. excessive reduction of the filter length, does not necessarily work because there is no coupling evolution for the $I_y S_x$ term with respect to active spins during the filter.

It is noteworthy that if the magnitudes of $^1J_{I_1S}$ and $^1J_{I_2S}$ differ drastically from each other, like in a liquid crystal phase, the intensity imbalance between multiple quantum term and proton single quantum terms arise. This results in incomplete selection of $\alpha\beta$ and $\beta\alpha$ with respect to $\alpha\alpha$ and $\beta\beta$ spin-states (J cross-talk). Thus, by considering influence of J cross-talk on the measurement of $^2J_{HH}$, it can be realized that in the sum spectrum $\alpha\beta$ and $\beta\alpha$ lines are shifted towards each other due to deficient suppression of $\alpha\alpha$ and $\beta\beta$ lines. In contrast, the $\alpha\alpha$ and $\beta\beta$ lines are shifted away from each other due to incomplete cancellation of $\alpha\beta$ and $\beta\alpha$ lines (Figure 2). Therefore the measured $^2J_{HH}$ values are underestimates of their true values. The measured $^1J_{IS}$ values are not affected by the J cross-talk because $\beta\alpha$ lines are shifted in the same direction with respect to $\beta\beta$ lines, hence compensating the frequency shifts.

It is also worth pointing out that the proposed method can be very useful on samples at natural abundance, such as smaller proteins, or peptides thanks to very high sensitivity and artifact suppression capability of the experiment. Unsurprisingly, the passive carbon-carbon couplings are not problematic in these cases.

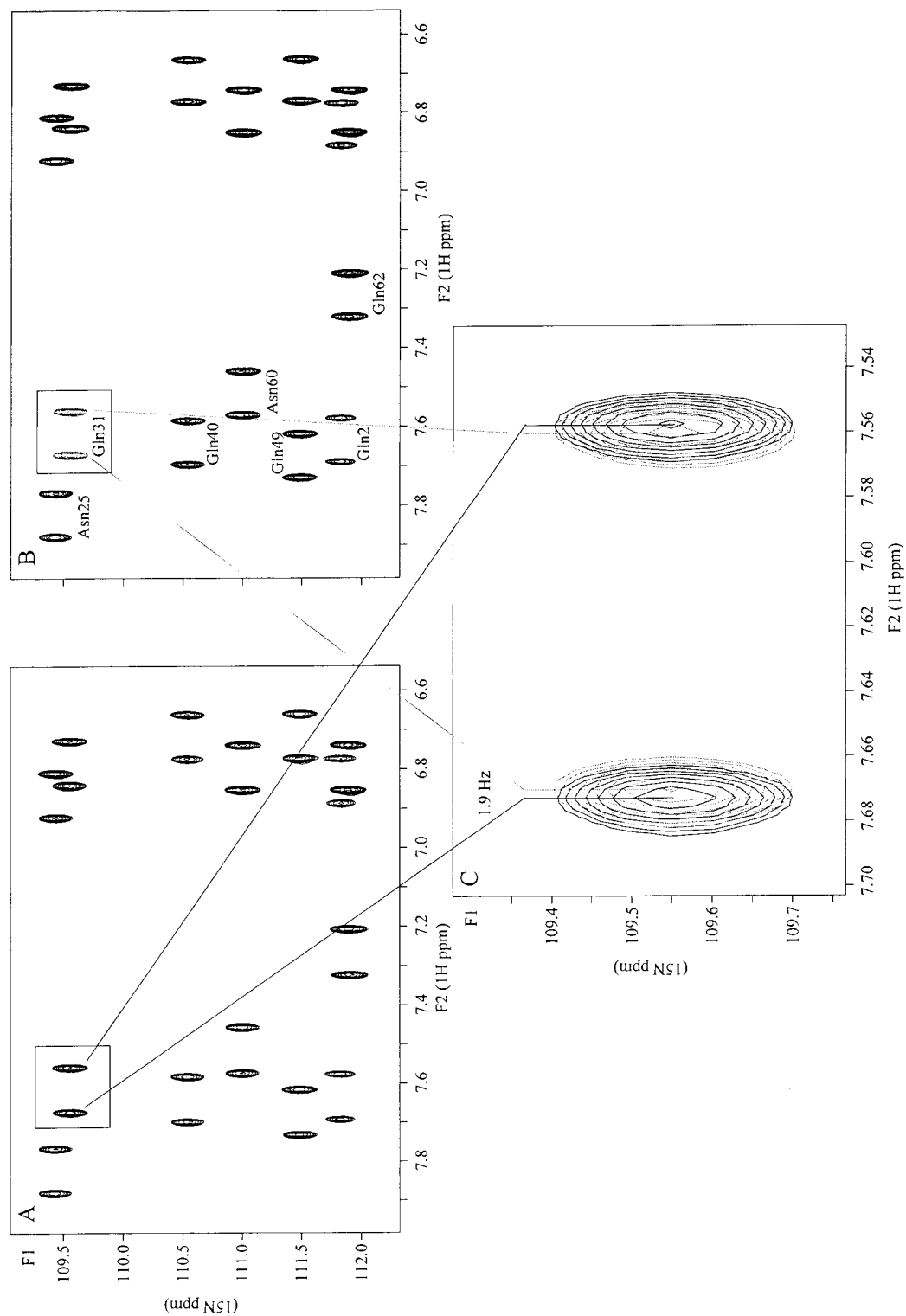


Figure 3. Representative expansions of ($\text{S}^3\text{-NH}_2$)-HSQC spectra recorded from 1.0 mM uniformly ^{15}N -labeled ubiquitin at 800 MHz ^1H frequency with the pulse scheme in Figure 1. The spectrum A and the spectrum B were collected using two phase settings for the last 90° (^{15}N) pulse: $\psi = x$ and $\psi = -x$, respectively. In C, expansion of Gln31 residue is shown for overlaid spectra A (black contours) and B (gray contours). Spectra were recorded with 128 and 1024 complex points using 2 transients per FID. Data were zero-filled to 1024x4096 data matrices and apodized with shifted squared sine-bell functions in both dimensions.

Table 1. Heteronuclear $^1J_{\text{HN}}$ and homonuclear $^2J_{\text{HH}}$ coupling constants found in ubiquitin as measured using the (S^3 -NH $_2$)-HSQC experiment

Residue	$^1J_{\text{H}^1\text{N}}$ [Hz]	$^1J_{\text{H}^2\text{N}}$ [Hz]	$^2J_{\text{H}^1\text{H}^2}$ [Hz]	$^2J_{\text{H}^2\text{H}^1}$ [Hz]
Gln2	90.9	88.7	2.3	2.3
Asn25	90.0	88.8	1.5	1.4
Gln31	90.3	88.6	1.9	1.8
Gln40	90.6	88.4	2.3	2.1
Gln41	86.9	89.4	2.3	2.3
Gln49	90.5	88.4	2.2	2.1
Asn60	91.1	88.9	2.3	2.2
Gln62	91.0	88.9	2.4	2.4

Figure 3 shows the representative expansion of NH $_2$ region of ubiquitin recorded using the (S^3 -NH $_2$)-HSQC pulse sequence in the Figure 1. The doublets in the spectrum A are resolved by the $^1J_{\text{H}^1\text{N}} + ^2J_{\text{H}^1\text{H}^2}$ ($^1J_{\text{H}^2\text{N}} + ^2J_{\text{H}^2\text{H}^1}$) whereas the splittings in F $_2$ in the spectrum B are resolved by the $^1J_{\text{H}^1\text{N}} - ^2J_{\text{H}^1\text{H}^2}$ ($^1J_{\text{H}^2\text{N}} - ^2J_{\text{H}^2\text{H}^1}$). Figure 3C shows the superposition of A and B spectra for the Gln31 residue, revealing the presence of minute coupling $^2J_{\text{HH}}$ (1.9 Hz). The exclusive spin-state-selection was achieved for all NH $_2$ resonances with no sign of spurious signals. The measured $^1J_{\text{NH}}$ and $^2J_{\text{HH}}$ couplings are listed on Table 1. The $^1J_{\text{NH}}$ couplings are in excellent agreement with our previous results with other proteins i.e., more deshielded proton has larger one-bond coupling to ^{15}N than the more shielded proton. Usually the downfield proton has $^1J_{\text{NH}}$ on the order of 90 ± 1 Hz, whereas the upfield proton has $^1J_{\text{NH}}$ in the 88 ± 1 Hz range. Although the difference is not striking, this tendency can also be found in other proteins (Permi, 2001). Interestingly, in ubiquitin there is one exception for this rule, Gln41, where the upfield proton has significantly larger $^1J_{\text{NH}}$ coupling (Table 1). The comparison of the measured $^2J_{\text{HH}}$ values with the previously determined values obtained by using the spin-state-selective DQ/ZQ experiment reveals that the new experiment has a bias towards smaller values. This may be explained by the fact that DQ/ZQ lineshapes are not purely absorptive (Permi et al., 1999a). The problem arises from the homonuclear coupling evolution (analogous to the HMQC experiment), which is active during t_1 and the polarization transfer delays and spin-state-selective filter element. This adds dispersive contribution into the lineshape complicating the measurement of couplings.

In the proposed experiment, the lineshapes are purely absorptive as in the familiar HSQC experiment.

Figure 4 shows the expansion of aliphatic $^{13}\text{C}/^1\text{H}$ region of ubiquitin, recorded using the (S^3 -CH $_2$)-HSQC experiment for proton-carbon correlation (Figure 1). The sum ($^1J_{\text{CH}} + ^2J_{\text{HH}}$) and difference ($^1J_{\text{CH}} - ^2J_{\text{HH}}$) spectra are superimposed revealing the quite large geminal coupling between the protons. For reference, the corresponding two CH $_2$ correlations, recorded using the conventional sensitivity enhanced ^{13}C -HSQC experiment without carbon decoupling during data acquisition, are shown within the boxed area above the overlaid sum and difference spectra (~ 1 ppm ^{13}C offset). This clearly illustrates that inner and outer lines are selected in the proposed experiment for the CH $_2$ groups. On the contrary, in the case of CH group at 50.5 ^{13}C ppm, there is no difference in the peak positions between the data from the regular HSQC (boxed area) and the data from the new experiment. The measured $^1J_{\text{CH}}$ and $^2J_{\text{HH}}$ couplings for the four CH $_2$ resonances are indicated in the spectrum. The corresponding $^1J_{\text{CH}}$ values obtained by using the ^{13}C -HSQC are in parenthesis.

It is commonly known that doublet components relax at different rates due to dipolar cross-correlation. In the CH $_2$ moiety, the proton H 1 will relax through the dipole-dipole interaction with directly bound ^{13}C . It will also relax through dipolar interaction with proximate protons, in this case especially due to the geminal pair H 2 . Careful analysis of the arising cross peaks in the Figure 4 reveals the effect of cross-correlation between these two relaxation pathways on the line widths of different multiplet components i.e., all four multiplet components have distinct line widths.

It is worth emphasizing that the new experiment retains the full sensitivity for the I $_2$ S moieties because

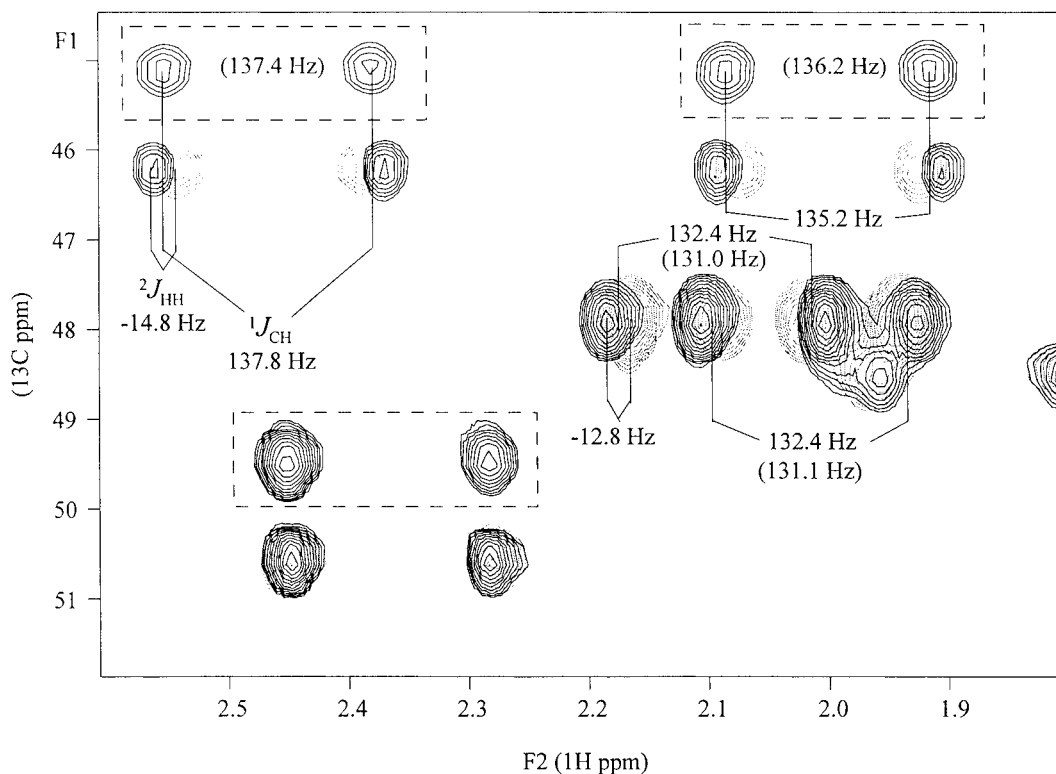


Figure 4. Expansions of the aliphatic region of (S^3 -CH₂)-HSQC spectra obtained from 0.8 mM uniformly $^{15}\text{N}/^{13}\text{C}$ enriched ubiquitin, measured at 800 ^1H MHz using the pulse sequence in Figure 1. The spectra recorded with the phase settings $\psi = x$ and $\psi = -x$ are shown superimposed. For a reference, expansions of the same resonances are shown in dashed boxes (for the sake of clarity these cross peaks are shifted ~ 1 ppm with respect to ^{13}C -axis), recorded using the conventional ^{13}C -HSQC without decoupling in F_2 . The spectrum displaying the doublet splittings equal to $^1J_{\text{CH}} + ^2J_{\text{HH}}$ is presented with black contours whereas the spectrum with multiplet splittings equal to $^1J_{\text{CH}} - ^2J_{\text{HH}}$ is shown with gray contours. The measured couplings $^1J_{\text{CH}}$ and $^2J_{\text{HH}}$ are marked in the figure. The $^1J_{\text{CH}}$ values obtained using the HSQC are in parenthesis. Experimental parameters for the (S^3 -CH₂)-HSQC experiment: Two spectra, $\psi = x$ and $\psi = -x$, were recorded with 256 and 1280 complex points using 8 transients per FID. Data were zero-filled to 1024x4096 data matrices and apodized with shifted squared sine-bell functions in both dimensions. The F_2 -coupled ^{13}C -HSQC experiment was recorded using the same parameters.

both coherence transfer pathways are preserved. Of course, the sensitivity is only half of the theoretical due to $^1J_{\text{IS}}$ coupling evolution during the acquisition. This approach provides the same sensitivity for I_2S moieties, that is gained using the conventional HSQC with $^1J_{\text{IS}}$ decoupling in both indirectly and directly detected dimensions. Comparison with the existing methods available for measuring coupling constants in the I_2S moieties, the proposed experiment provides very high sensitivity, and practical implementation is very simple. If only homonuclear two-bond couplings are going to be measured, the α/β -HSQC (Sattler et al., 1996) without gradient selection should give the optimal S/N. However, for the measurement of $^1J_{\text{IS}}$ (and $^1J_{\text{II}}$ inherently), the new experiment should give better S/N. On the other hand, the modified CBCA(CO)NNH experiment for the measurement of

$^1J_{\text{C}^\beta\text{H}^\beta}$, gives the optimum dispersion of cross peaks in the C^β sites but with significant loss in sensitivity. If the new experiment is employed for measuring the couplings in the I_2S moieties, it will double the number of resonances in the spectrum. This limits the applicability of the method for larger proteins, especially for methylene sites. In principle, the increase of cross peaks can be avoided by using the additional spin-state-selection. Thus, the 2ϵ period is increased to $1/(2J_{\text{IS}})$, and the two additional spectra are recorded with and without 180° pulse on ^{15}N (Figure 1). Consequently, the in- and antiphase spectra are generated that can be added or subtracted in a post-acquisition manner, resulting in only one multiplet component per subspectrum. When necessary, the (S^3 -NH₂)-HSQC scheme can be easily extended also to a three-dimensional (S^3 -NH₂)-HNCO corre-

lation experiment for improved dispersion, because the new method utilizes the familiar gradient selected, sensitivity-enhanced HSQC scheme (Kay et al., 1992). Alternatively, higher order NH₂ filtering can be exploited (Permi, 2001). The sufficient dispersion in the CH₂ region is much more difficult to obtain due to large number of resonances in the aliphatic region, especially on larger proteins. Fortunately, the proposed (S³-CH₂)-HSQC experiment can be easily modified to a constant-time (S³-CH₂)-CT-HSQC experiment, or to a three-dimensional experiment, which somewhat compensates for the increased number of cross peaks.

Conclusions

In conclusion, we have presented a simple two-dimensional NMR experiment enabling measurement of $^1J_{I_1S}$, $^1J_{I_2S}$, and $^2J_{I_1I_2}$, couplings in NH₂ or CH₂ sites of proteins and nucleic acids. Moreover, this new method also provides very high sensitivity for the I₂S moieties. Alternatively, if the measurement of $^1J_{IS}$ in the NH or CH spin systems is preferred, this can be accomplished by simply changing the phase of the last pulse on heteronucleus 90°. The ¹³C-edited version of the experiment should be very practical for smaller proteins and for samples at natural abundance in general, due to its high sensitivity and artifact suppression capability. We anticipate that the proposed method will be highly useful for acquiring information on protein side-chain orientation and dynamics.

Acknowledgements

This work was supported financially by the Ministry of Education. I thank the reviewers for their constructive and valuable comments.

References

- Andersson, P., Weigelt, J. and Otting, G. (1998) *J. Biomol. NMR*, **12**, 435–441.
- Annala, A., Aitio, H., Thulin, E. and Drakenberg, T. (1999) *J. Biomol. NMR*, **14**, 223–230.
- Bax, A. and Tjandra, N. (1997) *J. Biomol. NMR*, **10**, 289–292.
- Braunschweiler, G., Bodenhausen, G. and Ernst, R.R. (1983) *Mol. Phys.*, **48**, 535–541.
- Carlomagno, T., Peti, W. and Griesinger, C. (2000) *J. Biomol. NMR*, **17**, 99–109.
- Chou, J.J. and Bax, A. (2001) *J. Am. Chem. Soc.*, **123**, 3844–3845.
- Grzesiek, S. and Bax, A. (1993) *J. Am. Chem. Soc.*, **115**, 12593–12594.
- Kaikkonen, A. and Otting, G. (2001) *J. Am. Chem. Soc.*, **123**, 1770–1771.
- Kay, L.E., Keifer, P. and Saarinen, T. (1992) *J. Am. Chem. Soc.*, **114**, 10663–10665.
- Kontaxis, G. and Bax, A. (2001) *J. Biomol. NMR*, **20**, 77–82.
- Marion, D., Ikura, M., Tschudin, R. and Bax, A. (1989) *J. Magn. Reson.*, **85**, 393–399.
- Meissner, A., Duus, J.Ø. and Sørensen, O.W. (1997) *J. Biomol. NMR*, **10**, 89–94.
- Meissner, A., Schulte-Herbrüggen, T. and Sørensen, O.W. (1998) *J. Am. Chem. Soc.*, **120**, 7989–7990.
- Mittermaier, A. and Kay, L.E., (2001) *J. Am. Chem. Soc.*, **123**, 6892–6903.
- Ottiger, M., Delaglio, F. and Bax, A. (1998a) *J. Magn. Reson.*, **131**, 373–378.
- Ottiger, M., Delaglio, F., Marquardt, J.L., Tjandra, N. and Bax, A. (1998b) *J. Magn. Reson.*, **134**, 365–369.
- Otting, G., Rückert, M., Levitt, M.H. and Moshref, A. (2000) *J. Biomol. NMR*, **16**, 343–346.
- Parella, T. and Belloc, J. (2001) *J. Magn. Reson.*, **148**, 78–87.
- Permi, P. (2001) *J. Magn. Reson.*, in press.
- Permi, P. and Annala, A. (2000) *J. Biomol. NMR*, **16**, 221–227.
- Permi, P., Heikkinen, S., Kilpeläinen, I. and Annala, A. (1999a) *J. Magn. Reson.*, **139**, 273–280.
- Permi, P., Heikkinen, S., Kilpeläinen, I. and Annala, A. (1999b) *J. Magn. Reson.*, **140**, 32–40.
- Permi, P., Sorsa, T., Kilpeläinen, I. and Annala, A. (1999c) *J. Magn. Reson.*, **141**, 44–51.
- Permi, P., Rosevear, P.R. and Annala, A. (2000a) *J. Biomol. NMR*, **17**, 43–54.
- Permi, P., Kilpeläinen, I. and Annala, A. (2000b) *J. Magn. Reson.*, **146**, 255–259.
- Pervushin, K., Riek, R., Wider, G. and Wüthrich, K. (1997) *Proc. Natl. Acad. Sci. USA*, **94**, 12366–12371.
- Pervushin, K., Wider, G., Riek, R. and Wüthrich, K. (1999) *Proc. Natl. Acad. Sci. USA*, **96**, 9607–9612.
- Prestegard, J.H., Al-Hashimi, H.M. and Tolman, J.R. (2000) *Quart. Rev. Biophys.*, **33**, 371–424.
- Sattler, M., Schleucher, J., Schedletsky, O., Glaser, S.J., Griesinger, C., Nielsen, N.C. and Sørensen, O.W. (1996) *J. Magn. Reson.*, **A119**, 171–179.
- Tjandra, N. and Bax, A. (1997) *Science*, **278**, 1111–1114.
- Tjandra, N., Tate, S., Ono, A., Kainosho, M. and Bax, A. (2000) *J. Am. Chem. Soc.*, **122**, 6190–6200.
- Tolman, J.R., Flanagan, J.M., Kennedy, M.A. and Prestegard, J.H. (1995) *Proc. Natl. Acad. Sci. USA*, **92**, 9279–9283.
- Yang, D. and Nagayama, K. (1996) *J. Magn. Reson.*, **A118**, 117–121.
- Yang, D., Tolman, J.R., Goto, N.K. and Kay, L.E. (1998) *J. Biomol. NMR*, **12**, 325–332.
- Yang, D., Venters, R.A., Mueller, G.A., Choy, W.Y. and Kay, L.E. (1999) *J. Biomol. NMR*, **14**, 333–343.